

Effect of Sn Doping on the Properties of ZnO Thin Films Prepared by Spray Pyrolysis

Nadia Chahmat¹, Ammar Haddad¹, Azzedine Ain-Souya¹, Rachid Ganfoudi¹,
Nadir Attaf², Mouhamed Salah Aida², Mokhtar Ghers¹

¹Laboratory of Surfaces and Interfaces (LESIMS), Department of Physics, Faculty of Science,
University Badji Mokhtar of Annaba, Annaba, Algeria

²Laboratory of Thin Films Surfaces and Interface, Faculty of Science, Department of Physics,
University Mentouri of Constantine, Constantine, Algeria

Email: chahmatsou@yahoo.fr

Received July 26, 2012; revised September 3, 2012; accepted September 28, 2012

ABSTRACT

Layers of transparent and conductive Sn-doped zinc oxide (ZnO) have been prepared using chemical reactive liquid phase (spray) method on glass substrates. X-ray diffraction analysis shows that the obtained layers show preferential grains orientation along the direction (002). Microstructural analysis indicates that the thickness of the deposited films is independent of Sn content, *i.e.* 408 nm, and that the average grain size increases with increasing Sn content, ranging from 31 nm to 42 nm. The value of the optical gap obtained using UV-visible transmission spectroscopy method increases slightly from 3.1 eV to 3.3 eV. Moreover, transmission curves reveal that the prepared thin films are transparent in the visible domain.

Keywords: ZnO Thin Films; Ultrasonic Spray; Semiconductor Doping; Optical Gap

1. Introduction

Due to the excellent structural and optical properties, zinc oxide (ZnO) thin films have wide applications as solar cells [1], gas sensors [2], light emitting diodes (LED's), laser systems [3] and transparent electrodes [4]. Moreover, they can be prepared by different techniques, such as magnetron sputtering [5], reactive evaporation [6], chemical vapor deposition (CVD) [7], pulsed laser deposition (PLD) [8] and spray pyrolysis [9].

Among these methods, the spray pyrolysis technique has several advantages, such as, simplicity, safety, and low cost of the apparatus and raw materials.

Zinc oxide is a semiconductor with a direct large gap and generally, crystallizes in wurtzite structure [10]. However, the size, the orientation of grains and the surface quality depend on the conditions in which the material was prepared and the different treatments which can be made. Indeed, surface states of semiconductor materials generate superficial electronic properties which are often significantly affected by their interactions with foreign elements.

In the present study, we have investigated the effect of a larger Sn doping ratio range (up to 10%) on the structural and optical properties of tin doped zinc oxide thin films deposited by ultrasonic spray. Moreover, ZnO thin

films were deposited by ultrasonic spray technique with a non aqueous starting solution [11].

There have been extensive studies on the crystalline structure, optical transmittance of doped ZnO thin films prepared by spray pyrolysis methods [12]. There are, however, few studies on optical constants, and absorption coefficient of doped ZnO thin films. In this paper, we study the effect of different Sn percentages on the structural and optical properties of ZnO thin films deposited by spray pyrolysis.

2. Experimental

The films were grown onto glass substrates, using a typical spray pyrolysis system. The starting solution is composed with 0.1 molarity of zinc acetate ($\text{Zn}(\text{CH}_3\text{COO})_2 \cdot 2\text{H}_2\text{O}$) salt diluted in methanol. Sn doping is achieved by adding a small quantity of ($\text{SnCl}_2 \cdot 2\text{H}_2\text{O}$) in the solution. The weight of the added doping source is calculated as function of the desired Sn/Zn ratio. The latter was varied in the range of 0% - 10%. The prepared solution is then sprayed on the heated glass substrates by ultrasonic nebulizer system (Sonics) which transforms the liquid to a stream formed with uniform and fine droplets of 40 μm average diameter (given by the manufacturer). The temperature of the substrates was 350°C.

The spray pyrolysis method is one of the most commonly used methods for preparation of transparent and conducting oxides owing to its simplicity, safety, non-vacuum system of deposition and hence inexpensive method. Other advantages of the spray pyrolysis method are that it can be adapted easily for production of large-area films, and to get varying band gap materials during the deposition process.

The crystalline structure was studied by X-ray diffraction measurements using a Bruker D8 Advance diffractometer with Cu K α radiation ($\lambda_{Cu} = 0.154056$ nm). The diffractometer reflections were taken at room temperature and the value of 2θ were swapped between 20° and 70° . The optical transmission measurements were performed with a (UV-3101 PC-SHIMADZU) UV-Visible spectrophotometer. The thickness of the films was calculated from optical transmission by interference method.

3. Results and Discussion

3.1. Structural Properties

Figure 1 shows the spectra of X-ray diffraction for thin films of Sn doped and undoped. The peaks of X-ray diffraction indicate that all obtained films are polycrystalline with hexagonal wurtzite structure and a preferential orientation of c axis perpendicular to the substrate. There was no significant difference for the films undoped and Sn doped. Both kinds of spectra represent the dominant peak (002) which is located $2\theta = 34.09^\circ$ and 34.55° , respectively. Authors attribute this shift to the substitution of zinc and tin in the hexagonal structure. This result is in good agreement with literature data [13-15]. Another major orientation present is (100) and (101) are also seen in **Figure 1**.

It is also evident in **Figure 1** that the preferential (002) peak intensity increases with increasing Sn dopant concentration. This indicates an improvement in films crys-

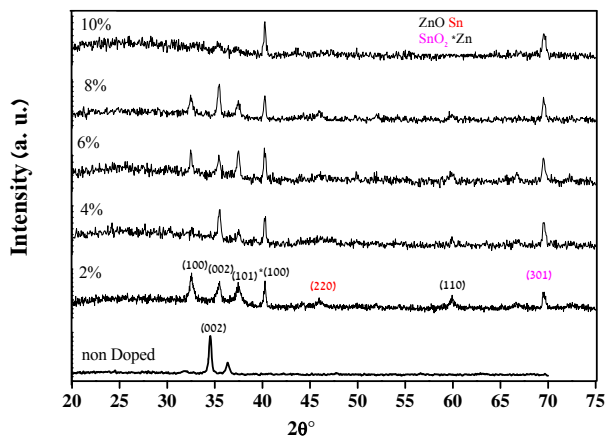


Figure 1. X-ray diffraction spectra of un-doped and Sn doped ZnO thin films.

tallinity with Sn film doping. However, for concentrations above 8% the films crystallinity is degraded [16] with Sn doping and the preferential orientation are changed from (002) to (101) and (100) [17,18]. This discrepancy may be due to the difference in the surface reactions.

The grain size of crystallites was calculated using a well-known Scherrer's formula [19]:

$$D = 0.9\lambda / \beta \cos \theta \quad (1)$$

where D is the grain size of crystallite, λ ($=1.54059$ Å) the wavelength of X-rays used, β the broadening of diffraction line measured at half its maximum intensity in radians and θ is the angle of diffraction. The values of grain size are found to be 31 nm to 41.37 nm for Sn doped ZnO and 29 nm for ZnO non doped thin films. **Figure 2** shows the variation of the grain size calculated from the X-ray diffraction patterns as mentioned in experimental section. The grain size of the films increases with different introduced percentages of the Sn.

3.2. Optical Properties

The optical properties of thin films of ZnO undoped and doped Sn was determined from the transmission measurement in the range of 300 - 800 nm. **Figure 3** shows the optical transmission of the doped films deposited onto the glass substrates. The transmission of the films changes with the Sn percentage doping. The properties of the films vary with the percentage of the doping element and this causes light loss on the films. Thus, the changes in the transmission take place. The fundamental absorption edge of the films corresponds to electron transitions from valence band to conduction band and this edge can be used to calculate the optical band gap of the films. The transmission decreases slightly when the percentage of Sn increases. All films show a high transmission in the UV-Vis and with a sharp absorption edge at 380 nm.

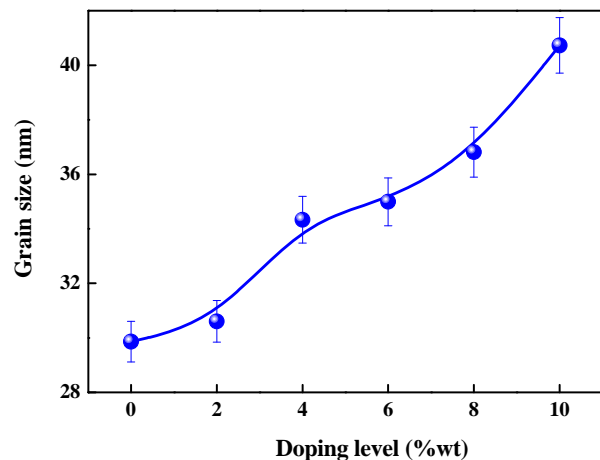


Figure 2. Variation of grain size with doping level.

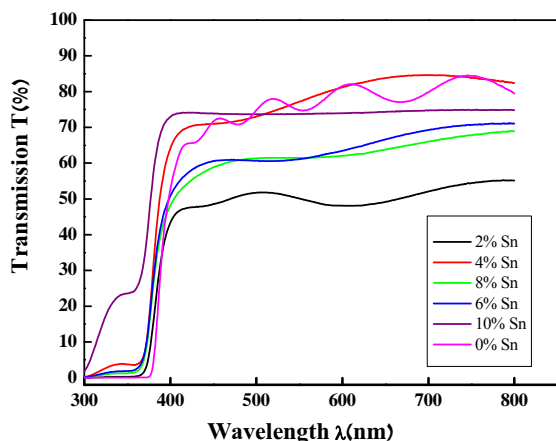


Figure 3. The transmittance spectra of un-doped and Sn doped ZnO thin films.

The absorption coefficient α of ZnO films was determined from transmittance measurements. The films absorption coefficient was calculated using the following expression:

$$\alpha = -(1/d)\ln(T) \tag{2}$$

where T is the normalized transmittance and d is the film thickness. These absorption coefficient values were used to determine optical energy gap. The energy gap (E_g) was estimated by assuming a direct transition between valence and conduction bands from the expression:

$$(\alpha h\nu) = A(h\nu - E_g)^{1/2} \tag{3}$$

where A is a constant, $h\nu$ is the photon energy and E_g is the optical band. **Figure 4** shows plots of $(\alpha h\nu)^2$ versus $(h\nu)$. The optical band gap of the films was calculated from these plots.

The Optical energy gap was derived assuming a direct transition between the edges of the valence band and the conduction band. The plot of $(\alpha h\nu)^2$ versus $(h\nu)$ gives by extrapolation of the linear region of the resulting curve the optical band gap value.

The calculated optical gap of samples increases with increasing the percentage of Sn from 3.256 eV for un-doped ZnO films to 3.3 eV for ZnO doped Sn. This shift of absorption of nanocrystalline films of ZnO doped Sn can be explained by the Burstein-Moss effect [20] while assuming the increase in carrier concentration that blocks the lowest states in the conduction band.

The absorption coefficient of films shows a tail for subband gap photon energy; this tail is so-called Urbach tail. The latter, which is closely related to the disorder in the film network, is expressed as [20]:

$$\alpha = \alpha_0 \exp(h\nu/E_U) \tag{4}$$

where α_0 is a constant, E_U is the Urbach energy, which characterizes the slope of the exponential edge. The

above equation describes the optical transition between occupied state in the valence band tail to unoccupied state of the conduction band edge. **Figure 5** shows Urbach plots of the films. The value of E_U was obtained from the inverse of the slope of $\ln\alpha$ versus $(h\nu)$. E_U values change inversely with optical band gap.

Figure 6 shows the variations of the optical gap together with the Urbach tail energy as a function of Sn doping level. It is clear that the optical gap is reduced with Sn doping. This band gap narrowing is due to the increase in the band tail width as shown in **Figure 6**. It is worth to bear in mind that the Urbach tail energy is closely related to the disorder in the film network. Since the ion radius of Sn is larger than Zn [20], the Sn introduction into the films is then followed by the lattice distortion and consequently disorder creation which cause the optical reduction. The same conclusion has been reported by A. Hafdallah *et al.* [11] in In doped ZnO.

The optical gap increases with the Sn doping concentration up to the percentage of 8%. Above this doping level, the gap value decreases. This shows that the percentage of 8% is the solubility limit of Sn in ZnO.

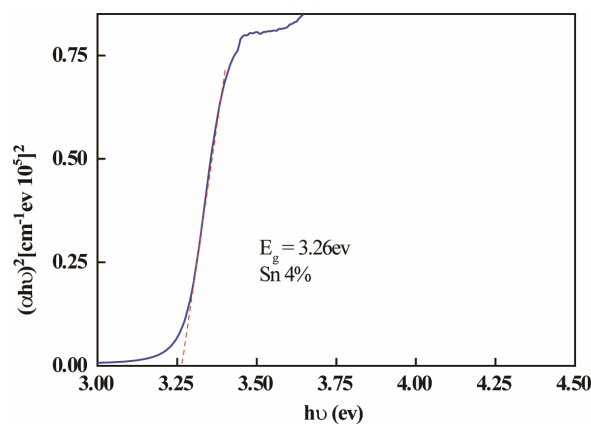


Figure 4. The plots of $(\alpha h\nu)^2$ as function of photon energy of the ZnO doped Sn.

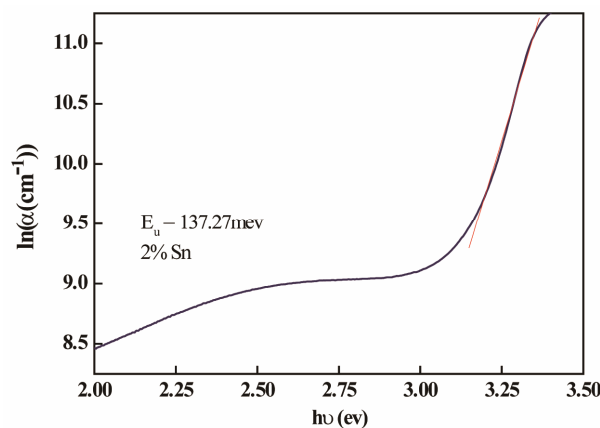


Figure 5. The Urbach plots of the doped thin ZnO.

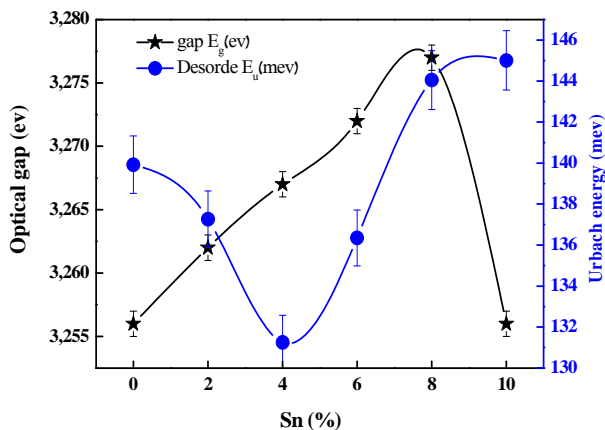


Figure 6. The effect Sn dopant on optical band gap and Urbach energy of the films.

4. Conclusions

ZnO thin films were deposited by ultrasonic spray technique with a non aqueous solution. The effect of Sn concentration on the structural and optical properties of films was investigated. The deposited films of ZnO undoped and doped Sn showed that the films have polycrystalline structure with preserve their (002) preferential orientation. The grain sizes increased depending on the increasing Sn concentration.

The optical transmission increases and becomes important for $\lambda > 380$ nm, which proves that the ZnO thin films Sn doped have an excellent transparency in the visible game while the optical gap is reduced with increasing in Sn/Zn doping ratio. This is linked to the disr with incorporation Sn in the film.

The optical gap of ZnO films increases with the percentage of Sn doping. When the limit of 8% doping is reached, the gap is reduced.

REFERENCES

- [1] J. B. Baxter and E. S. Aydil, "Dye-Sensitized Solar Cells Based on Semiconductor Morphologies with ZnO Nanowires," *Solar Energy Materials and Solar Cells*, Vol. 90, No. 5, 2006, pp. 607-622. [doi:10.1016/j.solmat.2005.05.010](https://doi.org/10.1016/j.solmat.2005.05.010)
- [2] S. T. Shishiyanu, T. S. Shishiyanu and O. I. Lupan, "Sensing Characteristics of Tin-Doped ZnO Thin Films as NO₂ Gas Sensor," *Sensors and Actuators B: Chemical*, Vol. 107, No. 1, 2005, pp. 379-386. [doi:10.1016/j.snb.2004.10.030](https://doi.org/10.1016/j.snb.2004.10.030)
- [3] J. M. Szarko, J. K. Song, B. C. W. Lackledge, I. Swart, S. R. Leone, S. Li, *et al.*, "Optical Injection Probing of Single ZnO Tetrapod Lasers," *Chemical Physics Letters*, Vol. 404, No. 1-3, 2005, pp. 171-176. [doi:10.1016/j.cplett.2005.01.063](https://doi.org/10.1016/j.cplett.2005.01.063)
- [4] T. Ootsuka, Z. Liu, M. Osamura, Y. Fukuzawa, R. Kuroda, Y. Suzuki, *et al.*, "Studies on Aluminum-Doped ZnO Films for Transparent Electrode and Antireflection Coating of β -FeSi₂ Optoelectronic Devices," *Thin Solid Films*, Vol. 476, No. 1, 2005, pp. 30-34. [doi:10.1016/j.tsf.2004.06.145](https://doi.org/10.1016/j.tsf.2004.06.145)
- [5] X. Yu, J. Ma, F. Ji, Y. Wang, X. Zhang and H. Ma, "Influence of Annealing on the Properties of ZnO: Ga Films Prepared by Radio Frequency Magnetron Sputtering," *Thin Solid Films*, Vol. 483, No. 1-2, 2005, pp. 296-300. [doi:10.1016/j.tsf.2005.01.013](https://doi.org/10.1016/j.tsf.2005.01.013)
- [6] J. Ma, F. Ji, D. Zhang, H. Ma and S. Li, "Optical and Electronic Properties of Transparent Conducting ZnO and ZnO: Al Films Prepared by Evaporating Method," *Thin Solid Films*, Vol. 357, No. 2, 1999, pp. 98-101. [doi:10.1016/S0040-6090\(99\)00357-0](https://doi.org/10.1016/S0040-6090(99)00357-0)
- [7] D. A. Lamb and S. J. C. Irvine, "Growth Properties of Thin Film ZnO Deposited by MOCVD with n-Butyl Alcohol as the Oxygen Precursor," *Journal Crystal Growth*, Vol. 273, No. 1-2, 2004, pp. 111-117. [doi:10.1016/j.jcrysgro.2004.08.027](https://doi.org/10.1016/j.jcrysgro.2004.08.027)
- [8] J. Zou, S. Zhou, C. Xia, Y. Hang, J. Xu, S. Gu, *et al.*, "Structural Optical and Electrical Properties of ZnO Films Grown on c-Plane Sapphire and (1 0 0) γ -LiAlO₂ by Pulse Laser Deposition," *Journal Crystal Growth*, Vol. 280, No. 1-2, 2005, pp. 185-190. [doi:10.1016/j.jcrysgro.2005.03.036](https://doi.org/10.1016/j.jcrysgro.2005.03.036)
- [9] P. Nunes, E. Fortunato, P. Tonello, F. Braz Fernandez, P. Vilarinho and R. Martins, "Effect of Different Dopant Elements on the Properties of ZnO Thin Films," *Vacuum*, Vol. 64, No. 3-4, 2002, pp. 281-285. [doi:10.1016/S0042-207X\(01\)00322-0](https://doi.org/10.1016/S0042-207X(01)00322-0)
- [10] A. A. EL-Fadl, G. A. Mohamed, A. B. Abd EL-Moiz and M. Rashad, "Optical Constants of Zn_{1-x}Li_xO Films Prepared by Chemical Bath Deposition Technique," *Physica B: Condensed Matter*, Vol. 366, No. 1-4, 2005, pp. 44-54.
- [11] A. Hafdallah, F. Yanineb, M. S. Aida and N. Attaf, "In Doped ZnO Thin Films," *Journal of Alloys and Compounds*, Vol. 509, No. 26, 2011, pp. 7267-7270. [doi:10.1016/j.jallcom.2011.04.058](https://doi.org/10.1016/j.jallcom.2011.04.058)
- [12] M. A. Lucio-López, M. A. Luna-Arias, A. Maldonado, M. de la L. Olvera and D. R. Acosta, "Preparation of Conducting and Transparent Indium-Doped ZnO Thin Films by Chemical Spray," *Solar Energy Materials and Solar Cells*, Vol. 90, No. 6, 2006, pp. 733-741. [doi:10.1016/j.solmat.2005.04.010](https://doi.org/10.1016/j.solmat.2005.04.010)
- [13] Y. Caglar, S. Ilican, M. Caglar and F. Yakuphanoglu, "Effects of Al and Sn Dopants on the Structural and Optical Properties of ZnO Thin Films," *Spectrochimica Acta Part A*, Vol. 67, No. 3-4, 2007, pp. 1113-1119.
- [14] J.-H. Lee and B.-O. Park, "Characteristics of Al-doped ZnO Thin Films Obtained by Ultrasonic Spray Pyrolysis Effects of Al Doping and an Annealing Treatment," *Thin Solid Films*, Vol. 426, No. 1-2, 2003, pp. 94-99. [doi:10.1016/S0040-6090\(03\)00014-2](https://doi.org/10.1016/S0040-6090(03)00014-2)
- [15] Z.-Q. Xu, H. Deng, Y. Li and H. Cheng, "Al-Doping Effects on Structure, Electrical and Optical Properties of c-Axis-Orientated ZnO: Al Thin Films," *Materials Science in Semiconductor Processing*, Vol. 9, No. 1-3, 2006, pp. 132-135. [doi:10.1016/j.mssp.2006.01.082](https://doi.org/10.1016/j.mssp.2006.01.082)
- [16] S. Ilican, Y. Caglar, M. Caglar and B. Demirci, "Polycrystalline Indium-Doped ZnO Thin Films: Preparation

- and Characterization,” *Journal of Optoelectronics and Advanced Materials*, Vol. 10, No. 10, 2008, pp. 2592-2598
- [17] S. Ilcan, Y. Caglar, M. Caglar and F. Yakuphanoglu, “Electrical Conductivity, Optical and Structural Properties of Indium-Doped ZnO Nanofiber Thin Film Deposited by Spray Pyrolysis Method,” *Physica E: Low-Dimensional Systems and Nanostructures*, Vol. 35, No. 1, 2006, pp. 131-138. [doi:10.1016/j.physe.2006.07.009](https://doi.org/10.1016/j.physe.2006.07.009)
- [18] M. A. Kaid and A. Ashour, “Preparation of ZnO-Doped Al Films by Spray Pyrolysis Technique,” *Applied Surface Science*, Vol. 253, No. 6, 2007, pp. 3029-3033. [doi:10.1016/j.apsusc.2006.06.045](https://doi.org/10.1016/j.apsusc.2006.06.045)
- [19] B. D. Cullity and S. R. Stock, “Elements of X-Ray Diffraction,” 3rd Edition, Prentice Hall, Upper Saddle River, 2001.
- [20] F. Paraguay, W. Estrada, D. R. Acosta, E. Andrade and M. Miki-Yoshida, “Growth, Structure and Optical Characterization of High Quality ZnO Thin Films Obtained by Spray Pyrolysis,” *Thin Solid Films*, Vol. 350, No. 1-2, 1999, pp. 192-202. [doi:10.1016/S0040-6090\(99\)00050-4](https://doi.org/10.1016/S0040-6090(99)00050-4)